

**DTA/TGA STUDY OF COPPER MOLYBDATE CARBOTHERMAL
REDUCTION**

S. V. AYDINYAN,¹ H. V. KIRAKOSYAN,¹ O. M. NIAZYAN¹ and S. L. KHARATYAN^{1,2}

¹A.B. Nalbandyan Institute of Chemical Physics NAS RA

5/2, P. Sevak Str., Yerevan, 0014, Armenia

²Yerevan State University

1, A. Manoukyan Str., Yerevan, 0025, Armenia

Email: a-sofya-1984@rambler.ru

The mechanism of copper molybdate carbothermal reduction was investigated at non-isothermal conditions by carrying out simultaneous differential thermal (DTA) and thermal-gravimetric (TGA) analyses combined with X-ray diffraction (XRD) analysis of intermediate and final products. In order to understand the influence of copper molybdate preparation method on the reduction processes, the behaviour of salts prepared by (i) calcination of oxides mixture and (ii) co-precipitation from water soluble salts of Cu and Mo were studied at linear heating. It was revealed that the obtained copper molybdates differ by modification and particle size distribution. Nevertheless, the reduction process of the both copper molybdates involves low-exothermic carbothermal reactions and is accompanied by sequential formation of partially reduced active phase $\text{Cu}_5\text{Mo}_6\text{O}_{18}$, as well as Cu_2O , MoO_2 , Cu and Mo. Chemical reactions possibly occurring during the heating of $\text{CuMoO}_4\text{-C}$ system on the basis of DTA/TG curves and XRD analyses results of quenched reaction products have been proposed.

Fig. 9, references 29.

Composite materials, which consist of two or more metals with distinctly different physicomechanical properties, are widely used due to their multiple functionalities. Among such type of materials Mo-Cu alloys have been attracted a great interest caused by the facts, that despite the significant difference in lattice parameters and high difference of melting points of metals, as well as their insolubility in both solid and liquid states, they form a material with absolutely new structure, where distinct particles of one metal are dispersing in a matrix of the other one forming so called pseudo-alloys [1-4]. These properties render Mo-Cu alloys widespread applications in heavy-duty electronic contacts, welding electrodes,

vacuum technology, military fields, aeronautics, portable apparatus and some other advanced fields [1-6].

Mo–Cu composites are generally fabricated by Cu infiltration in Mo skeleton or liquid phase sintering of Mo–Cu powder mixtures [7-12]. Since the Mo–Cu system exhibits mutual immiscibility or negligible solubility, Mo–Cu powder compacts show very poor sinterability, even by liquid phase sintering above the melting point of Cu. Moreover, in most of the applications, high-dense Mo–Cu materials with homogeneous microstructure are required for high performance, which is possible by applying ultra-fine and well-dispersed powders. During last decade several attempts have been successfully made to improve the sinterability of Mo-Cu composite powders [13-19]. These are mechanical alloying, adding sintering aids, as well as hydrogen co-reduction of oxides obtained from molybdenum and copper oxygen-containing compounds. The latter usually is performed at temperatures 800-1000°C with long duration (from 2 to 10 *hours*), which is energy consuming and accompanied with undesirable growth of Cu grains, as well as resulting in drastic decrease of process efficiency.

Taking into account disadvantages of the above described methods (energy and time consumption, low efficiency and low productivity, the complexity of microstructure and porosity regulation), for the manufacturing of Mo-Cu composite materials co-reduction of Mo and Cu oxides was performed in the combustion mode [20]. For this purpose the principle of thermo-chemical coupling of reactions was used applying Mg/C combined reducers [21]. The point is that magnesiothermal reduction of MoO₃/CuO oxides is a high caloric process and proceeds in combustion mode very violently. Meanwhile, carbothermal reduction process of metal oxides is low exothermic one and can't be realized in the combustion mode.

Undoubtedly, for the synthesis of Mo-Cu composite materials a special interest represents the reduction of metals from such compounds that contain both the metals, such as copper molybdates [17-19, 22, 23], in particular CuMoO₄. The latter is usually prepared by calcination of the mixture of copper and molybdenum oxides (in air, at 700 °C), or by co-precipitation of water soluble salts of copper and molybdenum.

The use of copper molybdate as a precursor has certain privileges in contrast to joint reduction of oxides mixture, because both metals are in the same crystalline structure and chemically bonded in the salt, thus the formation of more homogeneous composite is supposed. Besides the high surface area and additional reactivity generated from the thermal decomposition of salt-precursors will shorten the diffusion distances and result in sufficient diffusion activities promoting the synthesis reactions in every discrete grain of initial powders.

In this work for the reduction of copper molybdates the carbon is considered more appropriate especially in terms of providing low-temperature reduction processes of metals. Note that carbothermal reduction of Mo and Cu from copper molybdate, particularly for the preparation of Mo-Cu alloys, by the best of our knowledge, has never been studied.

Recently it was demonstrated the beauty of CuMoO_4 as a carbon black oxidation catalyst [24]. According to the work of P. G. Chigrin and co-authors catalytic combustion of carbon black in the presence of CuMoO_4 at 350–420°C occurs and is accompanied by ~5% weight loss of the sample according to the following reaction: $10\text{CuMoO}_4 + 3\text{C} = \text{Cu}_4\text{Mo}_5\text{O}_{17} + \text{Cu}_6\text{Mo}_5\text{O}_{18} + 2\text{CO}_2 + \text{CO}$, which corresponds to complete reduction of Cu^{2+} in CuMoO_4 into Cu^+ . Then the mixture of salts is oxidized in air up to CuMoO_4 . About more depth reduction processes there is no information in the literature.

In the present work investigation of the mechanism of carbothermal reduction of copper molybdate is carried out by thermal analysis method at non-isothermal conditions. The suggested approach allowed to explore stepwise nature of complex reactions in the CuMoO_4 -C system by carrying out simultaneous differential thermal (DTA) and thermal-gravimetric (TGA) analyses combined with X-ray diffraction (XRD) analysis of intermediate and final products. Possible mechanism of interaction in the CuMoO_4 -C system was proposed that may contribute to the estimation of optimum conditions of complete reduction of copper molybdate and preparation of Mo-Cu alloys in the case of using complex reducing mixtures.

Experimental

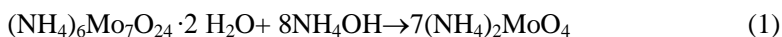
The following powders were used as raw materials: MoO_3 (High grade, Pobedit Company, Russia, particle size less than 15 μm), CuO (High grade, STANCHEM, Poland, particle size less than 40 μm), ammonium paramolybdate ($(\text{NH}_4)_6\text{Mo}_7\text{O}_{24}\cdot 4\text{H}_2\text{O}$, pure), copper sulphate ($\text{CuSO}_4\cdot 5\text{H}_2\text{O}$, pure), ammonium hydroxide (pure), and carbon black (P-803, Russia, particle size less than 1 μm).

Differential thermal (DTA) and thermogravimetric (TG) analyses were carried out using DTA/TGA, Q-1500 instrument (“Derivatograph Q1500” MOM, Hungary) which is connected to the multichannel acquisition system and output signals are recorded by a computer. Differential thermogravimetric (DTG) and DTA point were registered in every 1 s, samples 50-200 mg were placed in Al_2O_3 crucibles with 1 ml volume, Al_2O_3 powder was used as reference material. Measurements were conducted in argon (purity 99.97 %) atmosphere at flow rate of 120 ml/min. Heating rate was programmed to be 2.5, 5, 10, 20°C/min. The thermoanalytical curves were recorded up to a temperature 1000°C. In order to stop the reaction and quench the intermediate and final products for further investigations, the heater power was switched off automatically at preset temperatures, and the sample was cooled down by inert gas flow. The cooling rate in the temperature range from 1000 to 600°C (more interesting area) was around 300°C/min. The samples obtained in this way were examined by XRD with monochromatic $\text{CuK}\alpha$ radiation (diffractometer DRON-3.0, Burevestnik, Russia) operated at 25 kV and 10 mA. To identify the products from the XRD spectra, the data were processed using the JCPDS database. Microstructure of the initial mixture and intermediate and final products was

evaluated using Scanning Electron Microscope (SEM BS-300, Tesla, CZ) and Field Emission Scanning Electron Microscope Magellan 400 (FEI).

Copper molybdate preparation. Copper molybdate was prepared by two pathways. In the first case MoO_3 and CuO powders with a molar ratio of 1:1 were homogeneously mixed in a ceramic mortar and calcined in air at 700°C for 3 hrs (hereby as copper molybdate I). The obtained hard mass then was milled for 5 min using a Vibratory Mill machine (model 75T-DrM). After the milling process yellow-brown flour-like powder was obtained with $<300\text{ nm}$ average size (Fig. 1).

In the second case copper molybdate was prepared by chemical co-precipitation using $(\text{NH}_4)_6\text{Mo}_7\text{O}_{24}\cdot 2\text{H}_2\text{O}$ and $\text{CuSO}_4\cdot 5\text{H}_2\text{O}$ as starting materials. At first $\text{CuSO}_4\cdot 5\text{H}_2\text{O}$ was solved in deionized water to obtain aqueous solution of CuSO_4 , then $(\text{NH}_4)_6\text{Mo}_7\text{O}_{24}\cdot 2\text{H}_2\text{O}$ was converted into $(\text{NH}_4)_2\text{MoO}_4$ by the reaction with a proper quantity of ammonia. The mixing of aqueous solutions of $(\text{NH}_4)_2\text{MoO}_4$ and CuSO_4 result in chemical co-precipitation of CuMoO_4 . By controlling the pH value, the reaction can proceed according to the following equations:



The deposition rate of CuMoO_4 from two reacting solutions was controlled to produce a yellow-green precipitate which was dried in vacuum oven at 100°C . The results reveal that optimum conditions of the chemical co-precipitation are as follows: reaction temperature $50 \pm 5^\circ\text{C}$, pH value makes 5.1 ± 0.1 , and ageing time $9 \pm 1\text{ hrs}$.

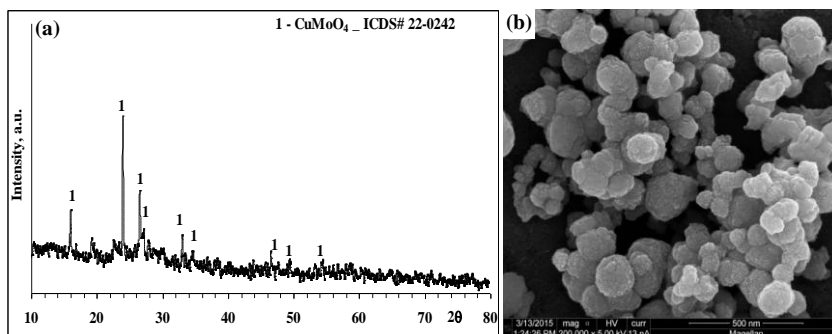


Fig. 1. XRD pattern (a) and SEM micrograph (b) of copper molybdate obtained by pathway I after 5 min milling.

Under the conditions mentioned above, average particle size of the prepared CuMoO_4 powder is less than 100 nm (fig.2b). Copper molybdates obtained by calcination and co-precipitation were characterized by XRD (fig. 1a, 2a), SEM (fig. 1b, 2b) and IR (figs. 3, 4) spectral analyses methods.

It should be noted that the copper molybdate (I) according to XRD and IR spectral analysis results presents as CuMoO_4 (Figs. 1a, 3).

According to XRD & IR spectral analyses results the salt obtained from solution (hereby as copper molybdate II) represents a mixture of copper molybdate (CuMoO_4) and hydroxymolybdate ($\text{Cu}_3(\text{MoO}_4)(\text{OH})_4$).

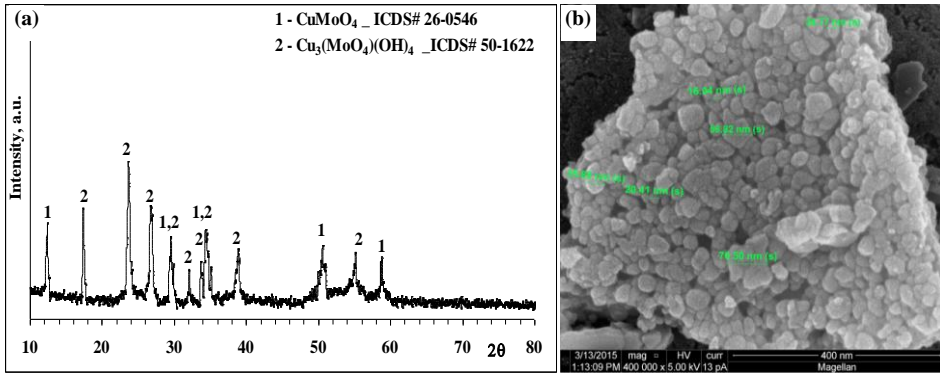


Fig. 2. XRD pattern (a) and SEM micrograph (b) of copper molybdate obtained by pathway II.

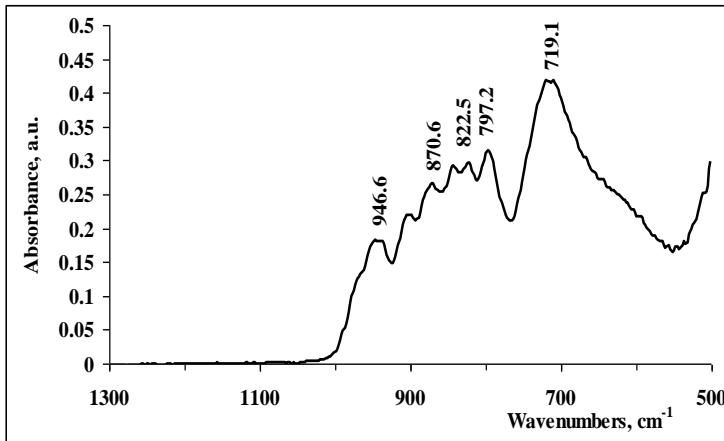


Fig. 3. IR spectra of copper molybdate obtained by pathway I.

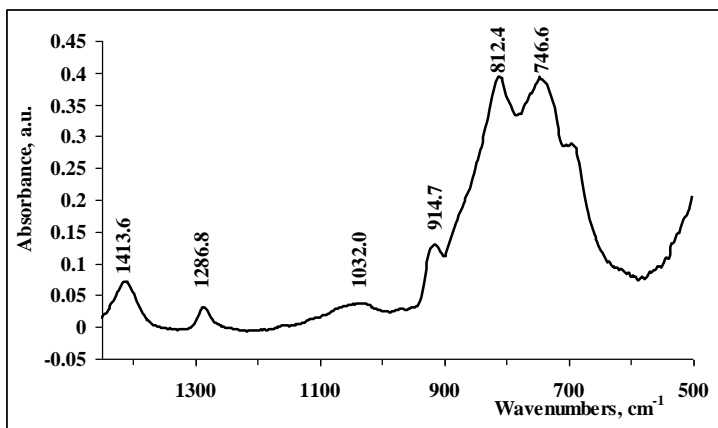


Fig. 4. IR spectra of copper molybdate obtained by pathway II.

Results and discussion

Firstly, behaviour of the both copper molybdates was studied at linear heating. As it can be seen from DTA/TG curves (Fig. 5), the CuMoO_4 (I) up to 700°C ($V_h=20^\circ\text{C}/\text{min}$, $m_o=100\text{ mg}$) is stable and endothermic peak at that temperature (A point) corresponds to the change of copper molybdate modification (\square - CuMoO_4 to CuMoO_4 -III) [25-27].

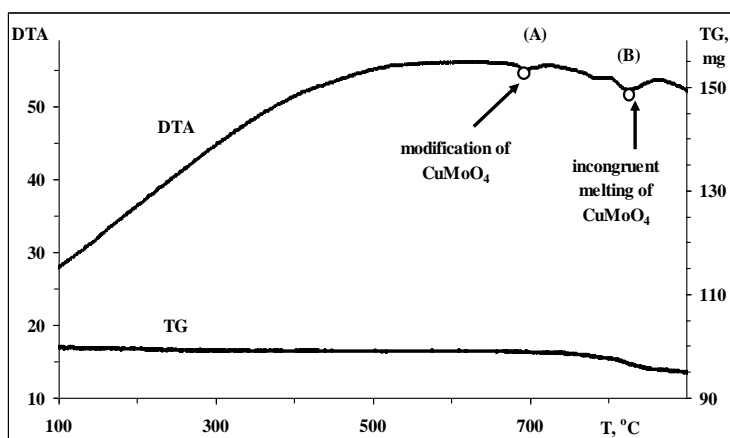


Fig. 5. DTA/TG curves of copper molybdate (I), $V=20^\circ\text{C}/\text{min}$, $m_o=100\text{ mg}$.

According to the literary data [28,29] at 820°C copper molybdate incongruent melting takes place (B point) followed by sublimation of the obtained molybdenum trioxide (this is evidenced by the weight loss on TG curve).

The investigation of thermal behaviour of copper molybdate (II) obtained from co-precipitation shows (fig. 6), that there are two endothermic stages at 250 - 310°C and 800 - 850°C temperature intervals.

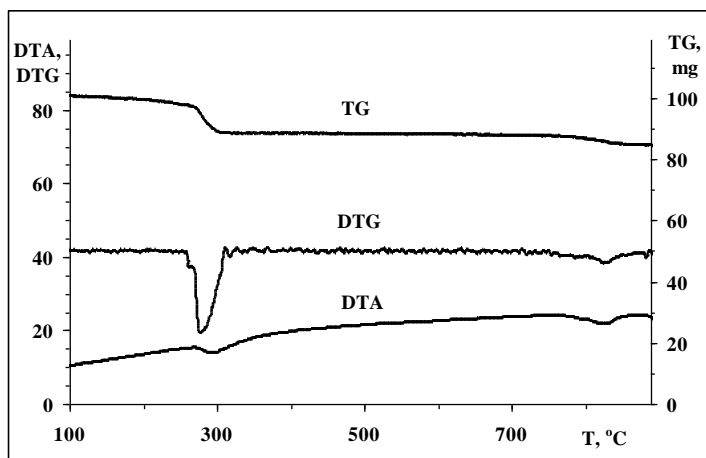


Fig. 6. DTA/DTG/TG curves of copper molybdate (II), $V=20^\circ\text{C}/\text{min}$, $m_o=100\text{ mg}$.

Thermal decomposition occurs followed by the mass change and XRD analysis of quenched samples indicate that the first stage ($\Delta m_{\text{exp}} = 12.5\%$) corresponds to the decomposition of copper hydroxymolybdate up to molybdate, whereas the second stage, which is also observed in the case of $\text{CuMoO}_4(\text{I})$, corresponds to the melting of copper molybdate(II) which is accompanied by salt's decomposition.

Carbothermal reduction of copper molybdates was investigated at linear heating conditions ($V_h = 20^\circ\text{C}/\text{min}$) in argon atmosphere (figs. 7 and 8). According to the results obtained, carbothermal reduction of copper molybdate is a multistage process. Particularly, as it can be seen from the DTA/TG curves of the $\text{CuMoO}_4(\text{I}) + 2\text{C}$ mixture notable changes aren't observed up to 470°C . In the $470\text{--}510^\circ\text{C}$ temperature interval copper oxide reduction takes place followed by molybdenum trioxide reduction ($540\text{--}610^\circ\text{C}$) up to MoO_2 , and above 800°C molybdenum dioxide partial reduction occurs.

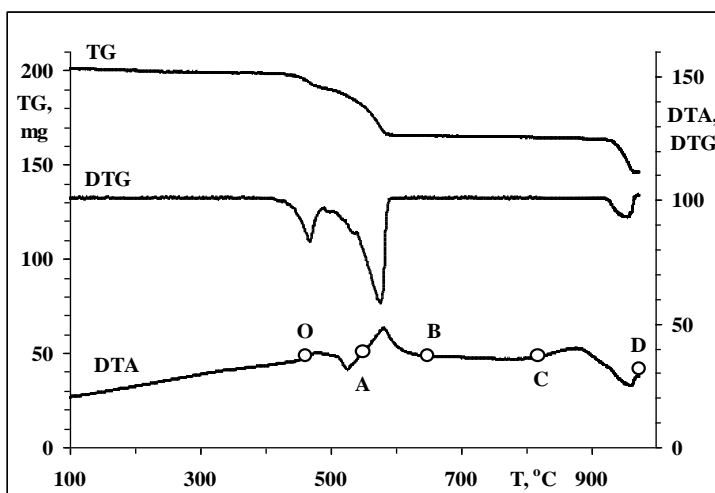


Fig 7. DTA/DTG/TG curves of the $\text{CuMoO}_4(\text{I}) + 2\text{C}$ mixture, $V = 20^\circ\text{C}/\text{min}$, $m_0 = 200\text{ mg}$.

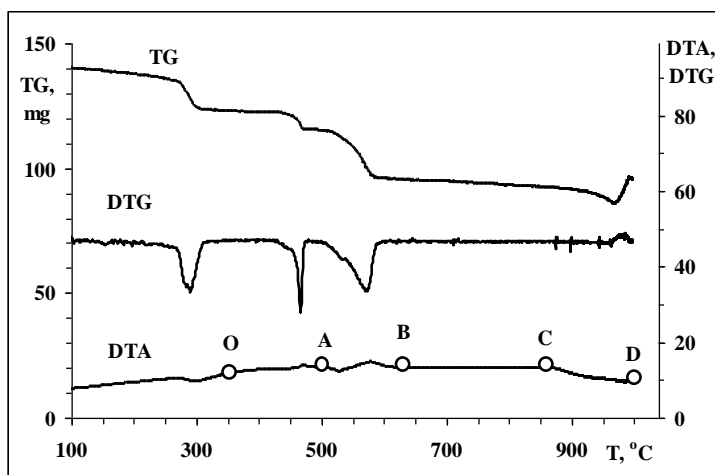


Fig 8. DTA/DTG/TG curves of the $\text{CuMoO}_4(\text{II}) + 2\text{C}$ mixture, $V = 20^\circ\text{C}/\text{min}$, $m_0 = 130\text{ mg}$.

As it can be seen from XRD analysis of the quenched samples obtained from characteristic temperatures (fig. 9), at 500°C the reduction product contains partially reduced copper molybdate with more complex structure ($\text{Cu}_5\text{Mo}_6\text{O}_{18}$), small amounts of copper suboxide and molybdenum dioxide are also present. At 625°C interaction leads to the complete reduction of copper and formation of MoO_2 . During the next stages ($>800^\circ\text{C}$) certain portion of molybdenum dioxide is reduced up to metallic molybdenum.

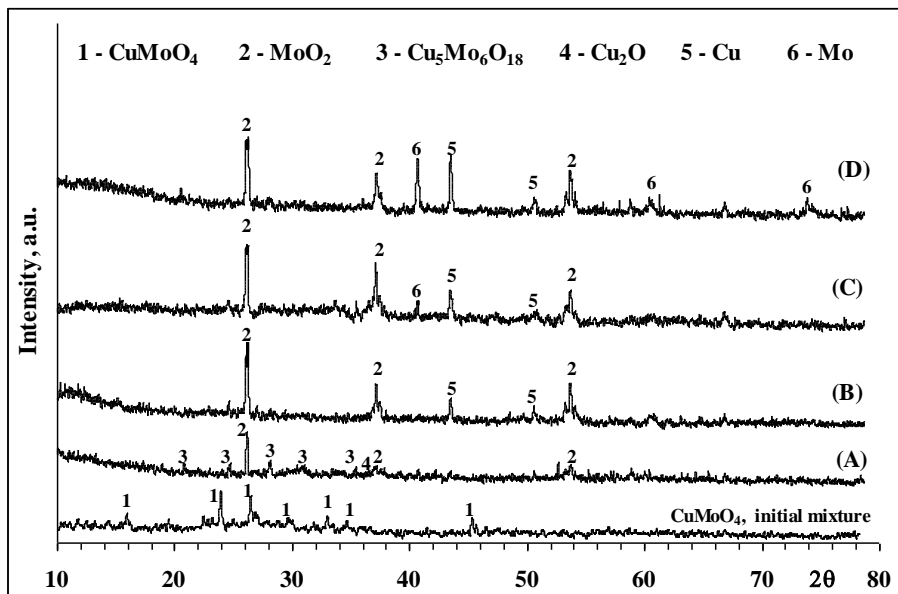
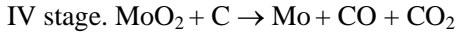
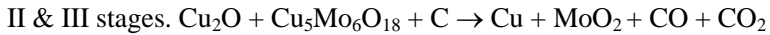


Fig. 9. XRD patterns of the intermediate products quenched from different characteristic temperatures: $\text{CuMoO}_4(\text{I})+2\text{C}$ reactive mixture. A – $T=500$, B – 625, C – 860, D – 970°C .

According to DTA/DTG/TG study of the $\text{CuMoO}_4(\text{II})+2\text{C}$ mixture (fig. 8), after the decomposition of copper hydroxymolybdate ($260\text{--}320^\circ\text{C}$) simultaneous decomposition and carbothermal reduction of copper molybdate occur at $430\text{--}490^\circ\text{C}$. Furthermore, in the temperature range of $510\text{--}600^\circ\text{C}$ first stage of carbothermal reduction of MoO_3 is observed. Then, at higher temperatures ($>800^\circ\text{C}$) MoO_2 partially reduces to molybdenum. This is evidenced by the both weight loss values and XRD analysis results of the quenched samples. The main differences between the carbothermal reduction processes of these two salts obtained by calcination and co-precipitation methods are the decomposition stage for copper molybdate (II) and carbothermic reduction processes of CuMoO_4 (II) shifted to the low temperature range about 50°C . Comparatively higher reactivity of copper molybdate (II) may be conditioned by the more fine-grained structure in comparison with CuMoO_4 (I).

Based on the results obtained, possible mechanism of carbothermal reduction of copper molybdate at linear heating conditions was outlined. According to the data obtained, salt decomposition into oxides and first stage-reduction processes start simultaneously. The subsequent reduction stage is complete reduction of copper and

formation of MoO_2 . This latter partially reduces to metallic molybdenum in the final stage.



The interaction pathway in the $\text{CuMoO}_4\text{-C}$ system was explored by thermal analysis method combined with XRD analysis of quenched intermediate and final products. It was shown that copper molybdates obtained by calcination and and coprecipitation are characterized by different phase composition and particle size. It was revealed that reduction process of the both copper molybdates involves low-exothermic carbothermal reactions which start with salt decomposition into oxides and simultaneous reduction up to formation of $\text{Cu}_5\text{Mo}_6\text{O}_{18}$, Cu_2O , MoO_2 , Cu and Mo . At the reduction of copper molybdate (II) temperature shift about 50°C was observed in the direction of low temperature range.

Acknowledgement

The authors acknowledge the financial support of the State Committee of Science of the Republic of Armenia (Project #13_1D192). Authors also would like to thank Dr. T.S. Kurtikyan for performing IR spectral analyses and Dr. Kh.V. Manukyan for performing SEM analyses of copper molybdates.

ՊՂՆՁԻ ՄՈՒԻԲՂԱՏԻ ԿԱՐԲՈՒԹԵՐՄ ՎԵՐԱԿԱՆԳՆՄԱՆ ՆԵՏԱԶՉՈՏՈՒԹՅՈՒՆԸ ԴԵՐԻՎԱՏՈԳՐԱՖԻԱԿԱՆ ԵՂԱՆԱԿՈՎ

Ս. Վ. ԱՅԳԻՆՅԱՆ, Ն. Վ. ԿԻՐԱԿՈՍՅԱՆ, Օ. Մ. ՆԻԱԶՅԱՆ և Ս. Լ. ԽԱՌԱՏՅԱՆ

Աշխատանքում ներկայացված է պղնձի մոլիբդատի՝ ածխածնով վերականգնման մեխանիզմի ուսումնասիրության արդյունքները ոչ իզոթերմ պայմաններում դիֆերենցիալ ջերմային և ջերմային զանգվածաչափական անալիզի եղանակներով: Ստացված տվյալները համադրվել են $\text{CuMoO}_4\text{-C}$ համակարգում փոխազդեցության միջանկյալ նյութերի և արգասիքների ռենտգենաֆազային անալիզի արդյունքների հետ: Պղնձի մոլիբդատի ստացման եղանակի ազդեցությունը վերականգնման գործընթացների վրա պարզաբանելու նպատակով հետազոտվել է օդում պղնձի ու մոլիբդենի օքսիդների համատեղ շիկացումից և պղնձի ու մոլիբդենի լուծելի աղերի համատեղ նստեցումից ստացված պղնձի մոլիբդատների ջերմային վարքը դժային տաքացման պայմաններում: Յույց է տրվել, որ տարբեր եղանակներով ստացված պղնձի մոլիբդատները տարբերվում են ինչպես մոդիֆիկացիայով, այնպես էլ մասնիկների չափսով ու բաշխվածությամբ: Այնուամենայնիվ, այդ երկու տեսակի պղնձի մոլիբդատների դեպքում էլ կարթթերմ վերականգնման պրոցեսը ներառում է թույլ էկզոթերմ կարթթերմ վերականգնման փուլեր և ուղեկցվում է նախ մասնակի վերականգնված ակտիվ ֆազի՝ $\text{Cu}_5\text{Mo}_6\text{O}_{18}$ առաջացմամբ, ապա դիտվում է Cu_2O , MoO_2 , Cu և Mo ֆազերի հաջորդական առաջացում: Հիմնվելով DTA/TG կորերից ստացված տվյալների և տարբեր բնութագրական ջերմաստիճաններից ստացված նմուշների ռենտգենաֆազային անալիզի արդյունքների վրա, առաջարկվել է $\text{CuMoO}_4\text{-C}$ համակարգում փոխազդեցության հնարավոր մեխանիզմը:

ДТА/ТГ ИССЛЕДОВАНИЕ КАРБОТЕРМИЧЕСКОГО ВОССТАНОВЛЕНИЯ МОЛИБДАТА МЕДИ

С. В. АЙДИНЯН¹, А. В. КИРАКОСЯН¹, О. М. НИАЗЯН¹ и С. Л. ХАРАТЯН^{1,2}

¹ Институт химической физики им. А.Б. Налбандяна НАН Республики Армения
Армения, 0014, Ереван, ул. П. Севака, 5/2

² Ереванский государственный университет
Армения, 0025, Ереван, ул. А. Манукяна, 1

В работе представлены результаты изучения механизма карботермического восстановления молибдата меди в неизотермических условиях путем проведения одновременного дифференциального термического (ДТА) и термогравиметрического (ТГА) анализов в сочетании с рентгенофазовым анализом промежуточных веществ и конечных продуктов. Для того чтобы выявить влияние способа получения молибдата меди на восстановительные процессы, было исследовано поведение солей, полученных: (а) путем прокаливания смеси оксидов металлов и (б) соосаждением из водорастворимых солей меди и молибдена в условиях линейного нагрева. Было установлено, что полученные молибдаты меди отличаются как типом модификации, так и распределением размера частиц. Тем не менее, процессы восстановления обоих молибдатов меди включают слабозотермические карботермические реакции и сопровождаются формированием частично восстановленной активной фазы – $\text{Cu}_5\text{Mo}_6\text{O}_{18}$, а также последовательным образованием Cu_2O , MoO_2 , Cu и Mo . На основе кривых ДТА/ТГ и результатов рентгенофазового анализа закаленных продуктов взаимодействия предложена последовательность возможных химических реакций, происходящих при нагревании системы $\text{CuMoO}_4\text{-C}$.

REFERENCES

- [1] *Joseph R.D.* Copper and Copper Alloys, ASM International, 2001, p. 621.
- [2] *Dirks A.G., Broek J.J.* // J. Vac. Sci. Technol. A, 1985, v.3, p. 2618.
- [3] *Ziebert C., Stueber M., Leiste H., Ulrich S., Holleck H.* // Nanoscale PVD Multilayer Coatings, Encyclopedia of Materials: Science and Technology, 2011, p. 1.
- [4] *Chen G.Q., Wu G.H., Zhu D.Z., Zhang Q., Jiang L.T.* // Transactions of Nonferrous Metals Society of China (English Edition), 2005, v.15, p. 110.
- [5] *Chen G., Wu G., Jiang L., Zhu D., Sun D.* // Key Engineering Materials, 2007, v. 4, p. 2883.
- [6] *Belay O.V., Kiselev S.P.* // Physical Mesomechanics, 2011, v.14, №3-4, p. 145.
- [7] *Ruan T., Wang Z., Jiang G., Tang R.* // Fenmo Yejin Jishu, Powder Metallurgy Technology, 2011, v.29, №4, p. 250.
- [8] *John L.J. and Randall M.G.* // Metallurgical and Materials Transactions A, 2001, v. 32A, p. 605.
- [9] *Nizhenko V.I., Petrishchev V.Ya., Skorokhod V.V.* // Powder Metallurgy and Metal Ceramics, 2008, v.47, №3-4, p. 163.
- [10] *Hu B.Q., Bai P.K., Wang Y.Z.* // Gongneng Cailiao/Journal of Functional Materials, 2012, v.43, №8, p. 1031.

- [11] *Fan J., Chen Y., Liu T., Tian J.* // Rare Metal Materials and Engineering, 2009, v.38, №10, p. 1693.
- [12] *Li Z., Han S.L., Jiang Y.L., Zhao D.F., Meng F.* // Materials Science and Engineering of Powder Metallurgy, 2011, v.16, №5, 2011, p. 774.
- [13] *Martinez V.P., Aguilar C., Marin J., Ordonez S., Castro F.* // Materials Letters, 2007, v.61, p. 929.
- [14] *Aguilar C., Guzman D., Rojas P.A., Ordonez S., Rios R.* // Materials Chemistry and Physics, 2011, v.128, p. 539.
- [15] *Hu B.Q., Bai P.K., Cheng J.* // Journal of Functional Materials, 2010, v.41, №5, p. 837.
- [16] *Aguilar C., Ordonez S., Marin J., Castro F., Martinez V.* // Materials Science and Engineering A, 2007, v.464, p. 288.
- [17] *Peng S., Jigui Ch., Lei W., Jingsong Z., Yifang W., Yanbo C.* // J. Alloys & Comp., 2009, v.476, p. 226.
- [18] *Aokui S., Dezhi W., Zhuangzhi W., Xiuqi Z.* // J. Alloys & Comp., 2010, v. 505, p. 588.
- [19] *Li Z., Zhai Y.* // Rare Metal Materials and Engineering, 2010, v.39, №1, p. 6.
- [20] *Aydinyan S.V., Manukyan Kh.V., Kharatyan S.L.* // XII Int. Symposium on SHS, TX, USA, 2013, Book of abstracts, p. 100.
- [21] *Kharatyan S.L., Merzhanov A.G.* // Int. J. SHS, 2012, v.21, №1, p. 59.
- [22] *Ming Z., Jinshu W., Wei L., Meiling Z.* // Journal of Physics: Conference Series, 2009, p. 188.
- [23] *Kang Z., Chen W., Ding B.* // Rare Metal Materials and Engineering, 2005, v.34, №6, p. 990.
- [24] *Chigrin P.G., Lebukhova N.V., Ustinov A.Yu.* // Kinetics and Catalysis, 2013, v.54, №1, p. 76.
- [25] *Wiesmann M., Ehrenberg H., Miede G., Peun T., Weitzel H., Fuess H.* // Journal of solid state chemistry, 1997, v.132, p. 88.
- [26] *Ehrenberg H., Weitzel H., Paulus H., Wiesmann M., Wltschek G., Geselle M., Fuess H.* // J. Phys. Chem. Sol., 1997, v.58, p.153.
- [27] *Tali R., Tabachenko V.V., Kovba L.M., Demyanets L.N.* // Russ. J. I.Chem., 1991, v.36, p. 927.
- [28] *Nassau K., Shiever J.W.* // Journal of the American Ceramic Society, 1969, v.52, Issue 1, p. 36.
- [29] *Machej T., Ziolkowski J.* // Journal of Solid State Chemistry, 1980, v.31, Issue 2, p. 135.